

Optimization of Combined Deep Drawing and Electromagnetic Corner Fill Process of DP980 Steel Sheet ^{*}

M. K. Choi ¹, H. Huh ¹, N. Park ¹, C. G. Jung ², J. Nam ²

¹ School of Mechanical, Aerospace and Systems Engineering, KAIST, Daejeon, Korea

² Metal Forming Research Group, POSCO, Incheon, Korea

Abstract

DP980 steel sheet is one of advanced high strength steel sheets (AHSS) introduced in order to achieve both enhanced crashworthiness and lightweight design of auto-body. Due to its comparatively poor formability, the application of DP980 steel sheet to auto-body is limited with conventional deep drawing processes. One of remedies is a combined deep drawing and electromagnetic sheet metal forming process, which is one of the innovative forming methods to improve the formability. The process chosen in this paper consists of square cup drawing of DP980 1.2t steel sheet with punch radius of 30 mm firstly and electromagnetic corner fill process to reduce the radius to 10 mm.

This paper proposes an approach for numerical optimization of combined deep drawing and electromagnetic corner fill process of DP980 steel sheet. The numerical optimization was conducted by following procedures of optimization of electromagnetic forming force and coil design. Conventional square cup drawing analysis was conducted first and the target function and constraint function were established to minimize the deviation from an ideal shape without violating forming limits for optimization of the EMF force. Then, coil design was carried out for small loss of electrical power transmission. Numerical results and conclusions are demonstrated for the applicability of this combined forming process.

Keywords

Deep drawing, Electromagnetic, Numerical optimization

^{*} This work is based on the results of the POSCO research project; the authors would like to thank POSCO for its financial support.

1 Introduction

Auto industries recently make efforts to develop lightweight vehicles with improvement of crashworthiness of auto-body. Advanced high strength steels (AHSS) have been introduced in order to achieve both enhanced crashworthiness and lightweight design of auto-body. DP980 steel, one of AHSS materials, is a high strength steel with a micro-structure of a soft ferrite matrix containing islands of martensite as the secondary phase. Due to its comparatively poor formability, the application of DP980 steel sheet to auto-body is limited with conventional deep drawing processes.

Electromagnetic forming (EMF) is one of the innovative forming methods to improve the formability. EMF is a high-speed forming process that uses pulsed magnetic fields to apply induced forces by a transient high frequency current. EMF can be combined with conventional deep drawing to make a sharp corner radius of a workpiece that cannot be obtained by conventional deep drawing. Regarding the combined deep drawing and electromagnetic corner fill process, many researchers carried out experimental and numerical study over the last years. Psyk et al. [1] studied integration of electromagnetic calibration into the deep drawing process to sharpen edge corner and Imbert and Worswick [2] showed that hybrid conventional/EM forming process using a specially designed coil could be successful in forming features in aluminium alloy sheet parts. Taebi et al. [3] developed a method for the computer aided design of process chains consisting of quasi-static and EMF in order to increase the classical quasi-static forming limits.

However, most of research works about the process are only limited to the application of aluminium alloys. Generally, electromagnetic forming is suitable for materials with a high electrical conductivity and low flow stress in order to achieve small loss of electrical power transmission. The application of DP980 steel sheet to electromagnetic forming is more difficult than other high conductive materials since DP980 steel has low electrical conductivity and very high flow stress. Therefore, it is necessary to optimize the combined deep drawing and electromagnetic corner fill process for the application of DP980 steel sheet.

The objective of this paper is to propose the optimization of EM forming force and coil design in the process without violating forming limits and with small loss of electrical power transmission. This approach requires adequate process parameters so that a desired shape is formed as close as possible. Numerical simulations were conducted to optimize the process with a commercial code LS-dyna and related experiments were carried out for the mechanical properties and FLD of the material. Conventional square cup drawing analysis was carried out first, and then the optimization procedures were conducted to set up the target function and constraint function to minimize the deviation from an ideal shape without violating forming limits for optimization of the EMF force. Based on the required EMF force obtained from the previous optimization, coil design was conducted for small loss of electrical power transmission as a noble proposal. Numerical results with optimization demonstrate the possibility of application this combined forming process to practical forming of DP980 for auto-body members.

2 Procedures for numerical optimization of the process

Numerical simulation of the process is regarded as multistep analysis which consists of pre-forming analysis and EMF coupled analysis using the deformed sheet in the pre-forming analysis. Since there are many process parameters of EMF system, optimization of process parameters of the EMF system directly is rather time-consuming. Hence, numerical optimization carried out in this paper follows the systematic procedures explained in Figure 1 (a). According to the flow chart, a conventional pre-forming analysis is followed by optimization for EM corner fill forming force, and then the EM tool coil is designed.

2.1 Optimization for EM corner fill forming force

Process parameters of the EMF force were optimized since the amount of sharpening of corner radius can be different with applied forming force. To solve the optimization problem, an objective function is setup to minimize the deviation from an ideal shape without violating forming limits. The process parameters should be carefully chosen and a design of experiment (DOE) method is used to reduce the number of simulations. Optimization of the resultant forming force to sharpen the corner radius is conducted using response surface method (RSM) with selected process parameters. The objective function was approximated by a regression equation to seek for optimum process parameters. Figure 1 (b) shows schematic diagram of the optimization procedures of the forming force.

2.2 Design of the EM tooling

To realize the optimized forming force with small loss of energy transition, EM tool coil was designed. Coil design is one of the most important problems in EM forming since tool coil delivers the energy to the corner filling area to be formed. Tool coil is integrated in the punch of the square cup drawing. This design process is carried out with dimensional analysis.

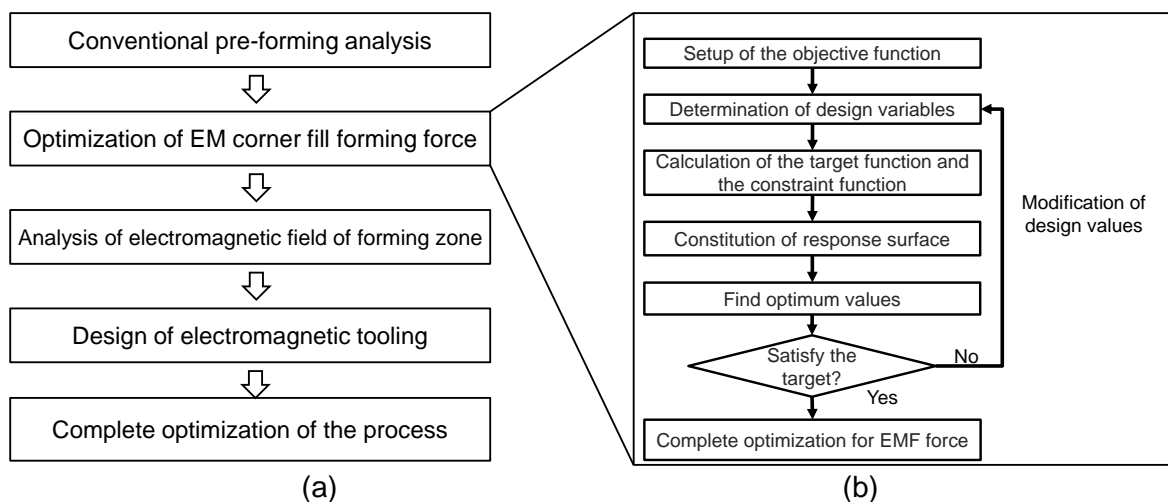


Figure 1: (a) Optimization procedures of the process; (b) schematic diagram of the optimization procedures of the forming force

3 Conventional square cup drawing analysis

FE analysis of conventional square cup drawing using a commercial code LS-Dyna is conducted as pre-forming analysis. Attempts are made to form the sheet with punch radius of 10 mm and 30 mm to check whether pre-forming is successful. The mechanical properties of DP980 1.2t steel sheet are obtained experimentally and strain paths of the material during pre-forming process are compared to predict the onset of fracture.

3.1 Mechanical properties of DP980 1.2t steel sheet

During combined deep drawing and electromagnetic corner fill process, a workpiece material exhibits high strain rates in the range of 10000 s^{-1} [4]. Therefore, strain rate effect on tensile properties of DP980 steel sheet is required to characterize the material behaviour. Uniaxial tensile tests were conducted at strain rates ranging from 0.001 s^{-1} to 100 s^{-1} . All conducted tensile tests were followed test procedures proposed by Huh et al. [5] to measure stress and strain with low uncertainties. For input data of numerical simulation of electromagnetic corner fill process, stress-strain relations with high strain rates in the range of 10000 s^{-1} could be obtained by extrapolating a strain rate dependent constitutive equation proposed by Huh et al. [6]. Lim-Huh model is a novel dynamic hardening model which is newly proposed to accurately express the change in the strain hardening with the change in the strain rate. The equation for Lim-Huh model is expressed as below:

$$\sigma(\varepsilon, \dot{\varepsilon}) = \sigma_r(\varepsilon) \cdot \frac{1 + q(\varepsilon) \cdot \dot{\varepsilon}^m}{1 + q(\varepsilon) \cdot \dot{\varepsilon}_r^m} \quad \text{where} \quad \sigma_r(\varepsilon) = K(\varepsilon + \varepsilon_0)^n, \quad q(\varepsilon) = \frac{q_1}{(\varepsilon + q_2)^{q_3}}$$

where $\dot{\varepsilon}_0 = 0.001 \text{ s}^{-1}$ is the reference strain rate. The material parameters K , ε_0 , n are determined by the flow stress at the reference strain rate and the parameter q and m show strain rate sensitivity as functions of strain. Figure 2 (a) shows uniaxial tensile test results and Figure 2 (b) shows deviations of flow stress of Lim-Huh model from the measured data. Extrapolated data from Lim-Huh model could be used as input data of numerical simulations.

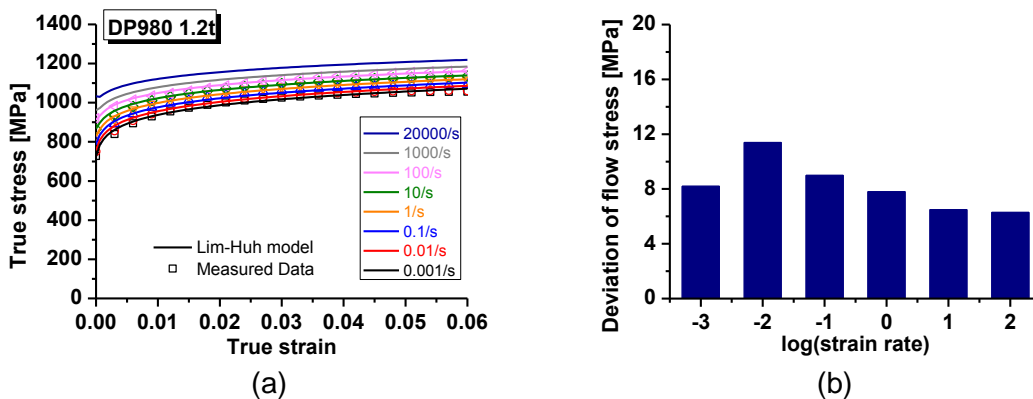


Figure 2: Tensile test results of DP980 steel sheet (a) true stress-true strain measured data and Lim-Huh model fitted curve (b) deviation of flow stress of Lim-Huh model

Consideration of fracture forming limits of the sheet is necessary to predict whether onset of fracture is observed during the process in the numerical optimization. Recently, Park et al. [7] have constructed a fracture forming limit diagram of DP980 steel sheet with fracture strains experimentally obtained at various loading paths. However, the fracture forming limit diagram is not able to account for the change of loading path during the process and the fracture forming limit diagram is not suitable to predict the onset of fracture during the process. Stoughton et al. [8] proposed a new strain-based forming limit criterion based on a polar diagram of the effective plastic strain with the direction defined by the arctangent of the ratio of the current plastic strain rates. This diagram is referred as the PEPS diagram in reference to its polar nature and its radial variable defined by the effective plastic strain, and has advantages that there is no dependence on the change of loading path and the stress-strain relation. Strain paths in major and minor strain space can be transformed to fracture based PEPS diagram by calculating the strain path as a function of θ and its corresponding equivalent plastic strain using the equation given below.

$$\bar{\varepsilon}_{pm} = \frac{1+r}{\sqrt{1+2r}} \sum_{i=1}^n \sqrt{(\Delta\varepsilon_{1i})^2 + (\Delta\varepsilon_{2i})^2} + \frac{2r}{1+r} (\Delta\varepsilon_{1i})(\Delta\varepsilon_{2i})$$

$$\theta_n = \tan^{-1} \left(\frac{\Delta\varepsilon_{2n}}{\Delta\varepsilon_{1n}} \right) \Rightarrow (x_n, y_n) = (\bar{\varepsilon}_{pm} \sin(\theta_n), \bar{\varepsilon}_{pm} \cos(\theta_n))$$

In this paper, a fracture based PEPS diagram is used as a fracture criterion to predict the onset of fracture during the process in the numerical simulation.

3.2 Finite element model and analysis condition

The stamping tool used for the pre-forming consists of a punch, die and blank holder. Figure 3 (a) shows an assembly of finite element models and figure 3 (b) shows dimensions of each part. The punch, die and holder are modelled with shell elements and treated as rigid surface.

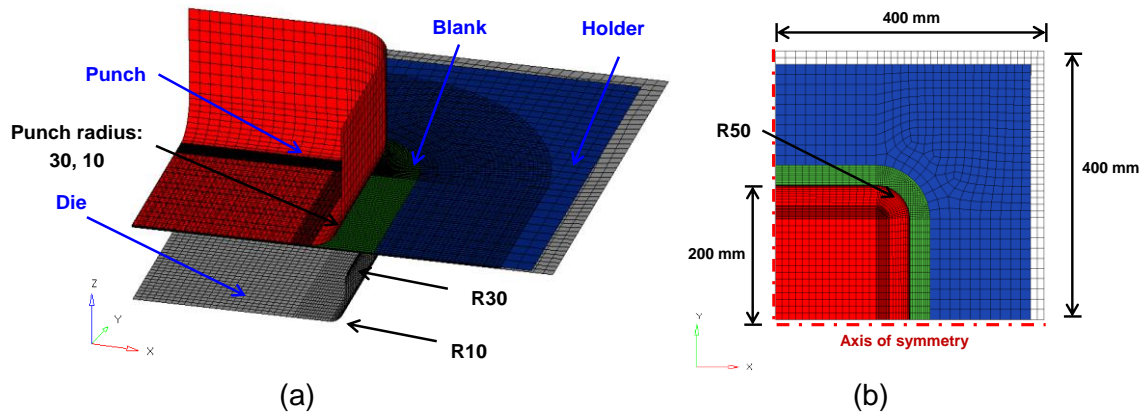


Figure 3. Finite element model for pre-forming analysis: (a) assembly of finite element models; (b) dimension of each part

The blank is modelled with 73325 8-node reduced integration solid elements with five elements along the through thickness direction since a solid element is required for EM coupled analysis. The stroke is set to 60 mm due to low formability of the material and the blank holding force given to the blank is 400 kN. The punch moves with 100 mm/s and friction coefficient of each contact surface is set to 0.1.

3.3 Analysis results

Strain paths of the material after the square cup drawing analysis with a punch radius of 30 and 10 mm are compared to predict the onset of fracture. Figures 4 (a), (b) show strain paths of 3 points at the punch corner, sidewall and die corner during the pre-forming in a fracture based polar EPS diagram. In this paper, it is determined that the onset of fracture is observed when any strain paths of a material exceed the fracture based polar EPS diagram of the material.

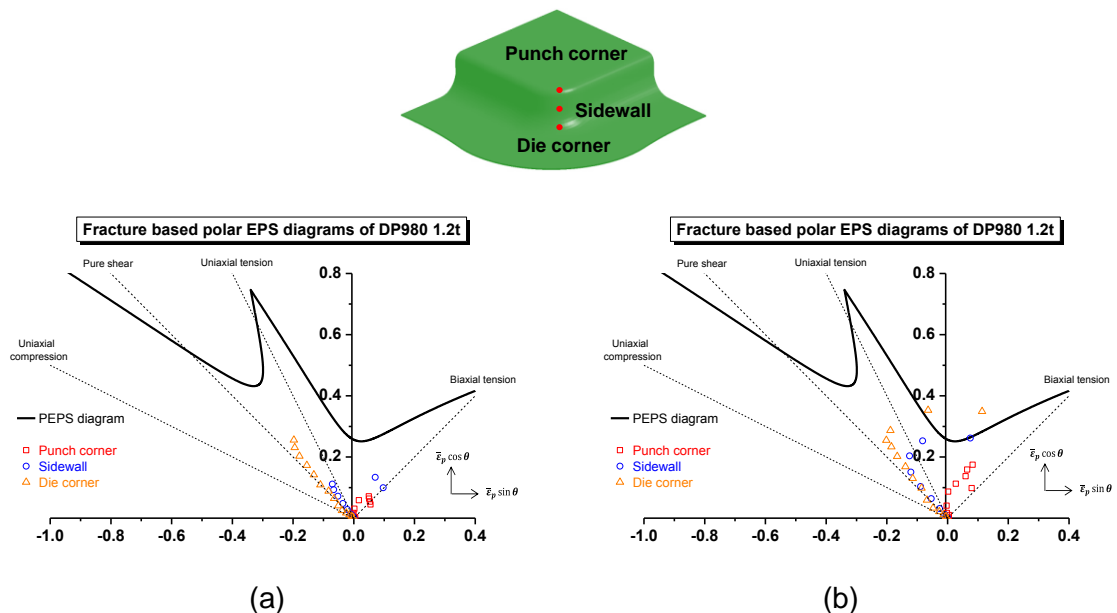


Figure 4. Strain paths during the square cup drawing analysis in fracture based PEPS diagram of: (a) punch radius 30 mm; (b) punch radius 10 mm

The simulation results show that all strain paths are under the PEPS diagram of the material in the case of a punch radius of 30 mm, which leads a conclusion that square cup drawing with punch radius of 30 mm is safe. On the other hand, the simulation results show that strain paths of the die corner and sidewall exceed the PEPS diagram of the material, which leads a conclusion that the onset of fracture is observed in the case of a punch radius of 10 mm. According to this analysis results, it is noted that the radius of 10 mm cannot be obtained with the conventional forming and an electromagnetic corner fill process is necessary to obtain the sharp radius of 10 mm in square cup forming by enhancing formability of the material.

4 Numerical optimization of the EM corner fill forming force

4.1 Determination of design variables

Numerical optimization of the EM corner fill forming force is carried out using numerical simulation of corner fill process by imposing forming force to a workpiece directly. Calibration zone where EM corner fill forming force is applied is indicated in figure 5 (a) and a forming force is imposed on the force imposed plane directly. To represent an imposed forming force as the Lorentz force electromagnetically induced as closely as possible, the damping factor and frequency are considered to assume that it is similar to the system current. Distribution of the imposed forming force on the force imposed plane is assumed to be non-uniform, but the force profile is a convex shape as well.

Process parameters to be optimized are selected as the total forming force, the angle of distributed area (θ_a) and the position of the force imposed plane (θ_p) which are defined in Figure 5 (b). The total forming force determines how much corner filling is achieved. Due to different stress state of the pre-formed workpiece at the calibration zone, the angle of distributed area (θ_a) and the position of the force imposed plane (θ_p) have influence on the final deformed shape and the formability of the material. Initial ranges of design values for each process parameter are shown below and 3 levels of process parameters are considered. Design values are updated during iterations of the optimization process.

Initial ranges of design values

- total forming force F : $1.8 \text{ MN} < F < 2.2 \text{ MN}$
- angle of distributed area θ_a : $20^\circ < \theta_a < 40^\circ$
- position of force imposed plane θ_p : $30^\circ < \theta_p < 60^\circ$

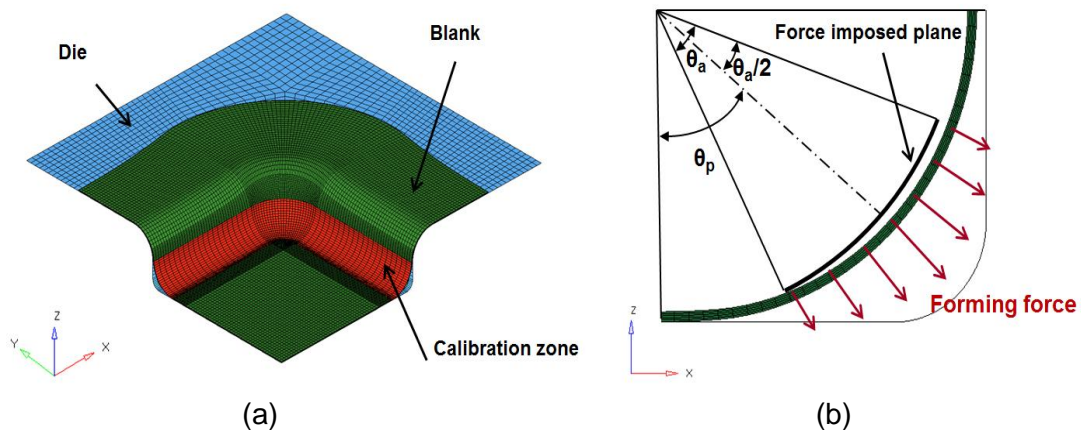


Figure 5: (a) Calibration zone EM corner fill forming force applied; (b) definition of the process parameters to be optimized

4.2 Objective function

Iteration of optimization procedure in Figure 1 (b) as mentioned in the previous chapter leads to the solution of the minimization problem which was introduced by Taebi et al. [3] as shown below:

$$\begin{aligned} &\text{minimize } f(\lambda_1, \dots, \lambda_n), \\ &\text{subject to } c(\lambda_1, \dots, \lambda_n, t) \geq 0 \end{aligned}$$

where f is the target function depending on n process parameters λ_k and it means the mean deviation of the shape of the deformed workpiece after a corner fill process from optimal geometry.

$$\begin{aligned} f(\lambda_1, \dots, \lambda_n) &= \left(\frac{1}{S_{zone}} \int_S |s(x, y, \lambda_1, \dots, \lambda_n) - s_{opt}(x, y)|^2 dx dy \right)^{\frac{1}{2}} \\ &= \left(\frac{1}{N} \sum_{k=1}^N |s(x_k, y_k, \lambda_1, \dots, \lambda_n) - s_{opt}(x_k, y_k)|^2 \right)^{\frac{1}{2}} \end{aligned}$$

where S_{zone} is the area of the calibration zone, $s(x, y, \lambda_1, \dots, \lambda_n)$ is the shape of the deformed blank, $s_{opt}(x, y)$ is the shape of optimal geometry which has a corner radius reduced to 10 mm and N is the number of nodes in the calibration zone. Integration is carried out over the whole surface of the calibration zone for the target function, but it can be considered as the mean deviation from nodes in the calibration zone.

The constraint function c is the minimum distance to the forming limits in the PEPS strain space at time t . The equation of the constraint function is shown below

$$c(\lambda_1, \dots, \lambda_n, t) = \min \left[(-1)^m \cdot \text{dist}((\bar{\varepsilon}_p \cos \theta(\lambda_1, \dots, \lambda_n, t), \bar{\varepsilon}_p \sin \theta(\lambda_1, \dots, \lambda_n, t)), F) \right]$$

$$\text{where } m = \begin{cases} 0, & \text{when forming limits are not violated} \\ 1, & \text{when forming limits are violated} \end{cases}$$

where $(\bar{\varepsilon}_p \cos \theta, \bar{\varepsilon}_p \sin \theta)$ is a point of strain path in the PEPS strain space and F is a fracture based PEPS diagram of the material. The constraint function c has negative value when forming limits are violated and thus the constraint function has to be positive for all time t .

4.3 Optimization result

The target function and the constraint function were calculated and approximated by response surface method to seek for optimum values of process parameters. Numerical simulations are carried out according to the Taguchi's L^9 orthogonal table since the analysis takes account of only the main effect of three process parameters. After the simulations, the response surfaces of the target function and the constraint function are approximated by the regression equation for optimum searching as follows:

$$\begin{aligned} f(x_1, x_2, x_3) &= \beta_0 + \beta_1 x_1 + \beta_2 x_2 + \beta_3 x_3 + \beta_4 x_1^2 + \beta_5 x_2^2 + \beta_6 x_3^2 \\ c(x_1, x_2, x_3) &= \beta_0 + \beta_1 x_1 + \beta_2 x_2 + \beta_3 x_3 + \beta_4 x_1^2 + \beta_5 x_2^2 + \beta_6 x_3^2 + \beta_7 x_1^3 + \beta_8 x_2^3 + \beta_9 x_3^3 \end{aligned}$$

where x_i and β_i are design values of each process parameter and the coefficients of the regression equation, respectively. Each regression equation is chosen to enhance the

approximation ability by adding the higher order terms in each regression equation. After response surfaces are constructed, optimum searching is conducted by solving the minimization problem in section 4.2. During the optimization process, the next iteration starts based on the design values of process parameters obtained from previous iteration until the converged values are acquired.

This optimization process converged after 4 iterations. A convergence criterion is the variation percentage of 1% for each process parameter. Figure 6 shows the optimum values of each process parameter and variation of the target function during the optimization process.

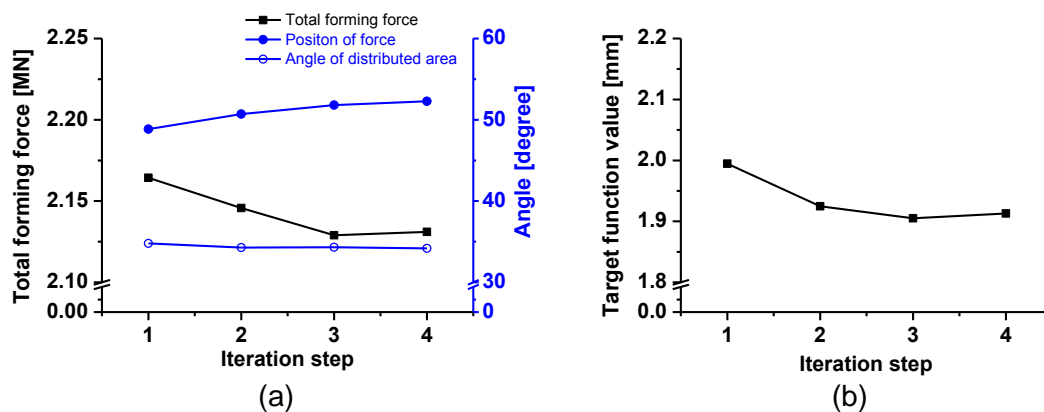


Figure 6: (a) Optimum values of each process parameter and (b) variation of the target function during the optimization process

5 Design of electromagnetic tool coil

After numerical optimization of the forming force, tool coil is designed, which is an important part delivering electromagnetic energy to the workpiece. The objective of this coil design is to realize the optimized forming force with small loss of energy transition.

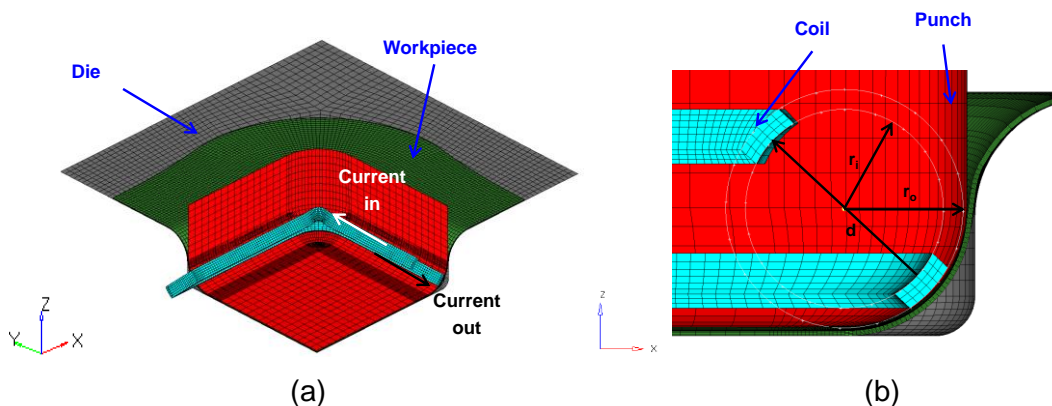


Figure 7: (a) Shape and location of the coil and (b) definition of the dimension of the tool coil

The type of an electro-magnetic tool coil for a successful corner fill process was studied by Imbert and Worswick [2] and the authors proposed U shape coil with the narrowed

section closest to a workpiece. In this paper, tool coil is designed with reference to the U shape with dimensional analysis. The shape and location of the coil are shown in Figure 7 (a). Coil dimensions for the angle of the force distributed area and the position of the tool coil located in the punch are determined from optimization results of EMF force. The gap between the punch and the coil is set to 1 mm.

Dimensional analysis is conducted numerically with various dimensions of the coil shown in Figure 7 (b) to compare the loss of energy transition. The effects of the coil thickness (r_o-r_i) and the distance between the upper and lower part of the coil (d) are also investigated. Numerical simulations are conducted using the LS-dyna EM module recently developed. The analysis time is 200 μs and input parameters representing EMF machine are the same for all analyses. The reference values of the dimension are selected as $r_o-r_i = 5$ mm and $d = 50$ mm. The normalized forming force exerted by the coil is compared with various dimensions in Figure 8.

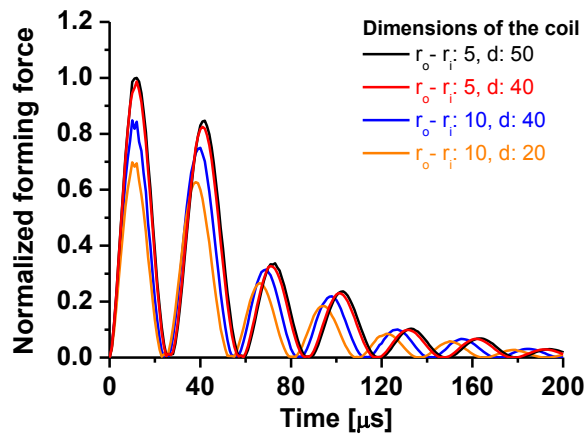


Figure 8: Normalized forming force with various dimensions of the tool coil

The forming force increases as the coil thickness decreases and the distance between the upper and lower part of the coil increases. Therefore, the coil designed with reference dimension has the smallest loss of energy transition among proposed designed coils. Using this coil, the required specifications of EMF machine regarded as an equivalent RLC circuit for the total forming force optimized can be calculated. The system resistance, the inductance and the capacity are supposed to be 6 m Ω , 230 nH and 380 μF respectively, the calculated charging voltage is 25 kV.

6 Conclusion

This paper proposes a systematic approach for numerical optimization of the combined square cup drawing and electromagnetic corner fill process, which is conducted to obtain process parameters for forming desired shape without violating forming limits. The strain rate dependent tensile properties and the strain path independent fracture forming limits are introduced for numerical simulation of the process. The optimization of the process is followed by an optimum design of the tool coil and required specifications of EMF system. It is noted that the combined deep drawing and electromagnetic corner fill process with DP980 steel sheet is possible for sharp corner edges with existing EMF machine to enhance the formability of the material. However, the required initial voltage for this process is larger than generally used values of EM forming for low strength materials and the feasibility of this process has to be proved by experiment. Moreover, the efficiency of the electromagnetic energy delivery would have to be enhanced to accommodate industrial settings.

References

- [1] *Psyk, V.; Beerwald, C.; Henselek, A.; Homberg, W.; Brosius, A.; Kleiner, M.:* Integration of Electromagnetic Calibration in to the Deep Drawing Process of an Industrial Demonstrator Part, *Key Engineering Materials*, Vol. 344, p. 435-442, 2007.
- [2] *Imbert, J.; Worswick, M.:* Electromagnetic reduction of a pre-formed radius on AA5754 sheet, *Journal of Materials Processing Technology*, 211, p.896-908, 2011.
- [3] *Taebi, F.; Demir, O.K.; Stiemer, M.; Psyk, V.; Kwiatkowski, L.; Brosius, A.; Blum, H.; Tekkaya, A.E.:* Dynamic forming limits and numerical optimization of combined quasi-static and impulse metal forming, *Computational Materials Science*, 54, p.293-302, 2012.
- [4] *Psyk, V.; Risch, D.; Kinsey, B.L.; Tekkaya, A.E.; Kleiner, M.:* Electromagnetic forming – A review, *Journal of Materials Processing Technology*, 211, p.896-908, 2011.
- [5] *Huh, H.; Jeong S.; Bahng G.W.; Chae K.S.; Kim C.G.:* Standard Uncertainty Evaluation for Dynamic Tensile Properties of Auto-Body Steel-Sheets, *Experimental Mechanics*, DOI 10.1007/s11340-014-9847-5
- [6] *Huh, H.; Ahn K.; Lim J. H.; Kim H. W.; Park L. J.:* Evaluation of dynamic hardening models for BCC, FCC, and HCP metals at a wide range of strain rates, *Journal of Materials Processing Technology*, 214, p.1326-1340, 2014.
- [7] *Park, N.; Ahn, K.; Lim, S. J.; Huh, H.:* Anisotropy Effect on the Fracture Model of DP980 Sheets Considering the Change of Loading Path. *Proceedings of the TUBEHYDRO 2013*, Jeju, Korea, August 26-28, 2013.
- [8] *Stoughton, T. B.; Yoon, J. H.:* Path independent forming limits in strain and stress spaces, *International Journal of Solids and Structures*, 49, p.3616-3625, 2012.

